

## Supplementary Materials for

### **Stromal Endothelial Cells Directly Influence Cancer Progression**

Joseph W. Franses, Aaron B. Baker, Vipul C. Chitalia, Elazer R. Edelman\*

\*To whom correspondence should be addressed. E-mail: ere@mit.edu

Published 19 January 2011, *Sci. Transl. Med.* **3**, 66ra5 (2011)

DOI: 10.1126/scitranslmed.3001542

#### **The PDF file includes:**

##### Materials and Methods

Fig. S1. Long-term culture of cancer cells in endothelial cell-conditioned media slows cell growth.

Fig. S2. Although the secretome of ECs contains a large amount of latent MMP2, it inhibits significantly cancer cell invasiveness.

Fig. S3. Media conditioned by normal fibroblasts have no effect on cancer cell proliferation or invasiveness.

Fig. S4. Inhibition of one signaling pathway in cancer cells cannot recapitulate EC-mediated regulation of cancer cells.

Fig. S5. Description of perlecan silencing on EC phenotype.

Fig. S6. Further studies of the perlecan/IL-6 axis in endothelial cells and its role in the regulation of cancer cell invasiveness.

Fig. S7. MEECs are phenotypically similar to ECs.

Fig. S8. Representative Ki-67 and S6RP staining in control and MEEC-treated A549 xenograft tumors.

Fig. S9. H&E-stained sections from each tumor showing intratumoral cysts.

Table S1. List of primers used for qRT-PCR.

## **Materials and Methods**

### ***Materials and Reagents***

Antibodies to Ki67 were from Santa Cruz Biotechnology, to NF- $\kappa$ B p65, p-S6RP, p-STAT3,  $\beta$ -actin, and MMP2 from Cell Signaling Technology, to PCNA from Abcam, and to IL-6 from RnD Systems. HRP-conjugated secondary antibodies were from Santa Cruz Biotechnology. Fluorescently-labeled secondary antibodies were from Invitrogen, rapamycin from Sigma, and DAPI and oligonucleotide PCR primers were from Invitrogen.

### ***Knockdown of perlecan in ECs***

pLKO.1 plasmids containing shRNA against perlecan, and as a control pLKO.1 without shRNA, (Open Biosystems, Huntsville, AL) were grown in transformed bacteria, purified (PureLink HiPure system, Invitrogen), and used to transfect HEK-293T packaging cells using Lipofectamine 2000 (Invitrogen). Packaging, envelope, and Rev plasmids were co-transfected simultaneously as described elsewhere (56). Viral particles were collected for 48 hours and transferred, along with 10  $\mu$ g/mL hexadimethrine bromide, to subconfluent EC monolayers. Puromycin (1  $\mu$ g/ml) was used for selection of stably transduced ECs.

### ***In vitro tube forming assay***

15,000 ECs were seeded in each well of 96-well plate coated with 50  $\mu$ L of Matrigel (BD Biosciences). After 16-20 hours, tube formation was imaged by phase contrast microscopy. ImageJ was used to quantify tube length, using 4 wells per condition.

### ***Gene expression analysis***

Total RNA was purified (RNEasy Mini Plus, Qiagen) and cDNA was synthesized (TaqMan reverse transcription reagents, Applied Biosystems) using 1  $\mu$ g of RNA. Real-time PCR analysis

was performed with an Opticon Real-Time PCR Machine (MJ Research) using SYBR Green PCR Master Mix (Applied Biosystems) and appropriate primers. Gene expression was quantified using the  $\Delta\Delta C_t$  method, with GAPDH as a housekeeping gene. Primer sequences are listed in Table S1.

### ***Protein expression and Western blotting***

Whole cell extracts were harvested with buffer containing 0.5% Triton X-100, 0.1% SDS, protease inhibitor cocktail (Roche), 2 mM sodium orthovanadate, 50 mM sodium fluoride, and 4 mM PMSF. Protein samples were separated on glycine-SDS gels, transferred to nitrocellulose membranes, immunoblotted with the appropriate primary and HRP-conjugated secondary antibodies, treated with a chemiluminescent peroxidase substrate (SuperSignal West Femto, Pierce). Luminescence was measured by a FluorChem luminometer (Alpha Innotech; CA) and analyzed using ImageJ. A cytokine antibody array (RayBiotech; GA) was used following the manufacturer's instructions for assessment of cell biosecretions. Array luminescence was imaged using a FluorChem luminometer (Alpha Innotech; CA) and quantified using ImageJ. IL-6 present in cell culture supernatants was assayed with an EIA kit (RnD Systems, Minneapolis, MN) according to the manufacturer's instructions.

### **Gelatin Zymography**

Samples were run on 10% polyacrylamide gels containing 0.1% gelatin (Invitrogen) under non-denaturing conditions. Recombinant human MMP2 (RnD Systems, Minneapolis, MN) was either used directly or after activation with 1 mM APMA (Sigma) and used as a control. Separated proteins were renatured with Triton X-100 (Invitrogen) and then allowed to digest the gelatin overnight at 37°C. Areas of gelatin digestion were detected by using a non-specific protein stain (Invitrogen) and the gels were scanned and analyzed using ImageJ.

### ***Immunofluorescent staining and epifluorescence microscopy***

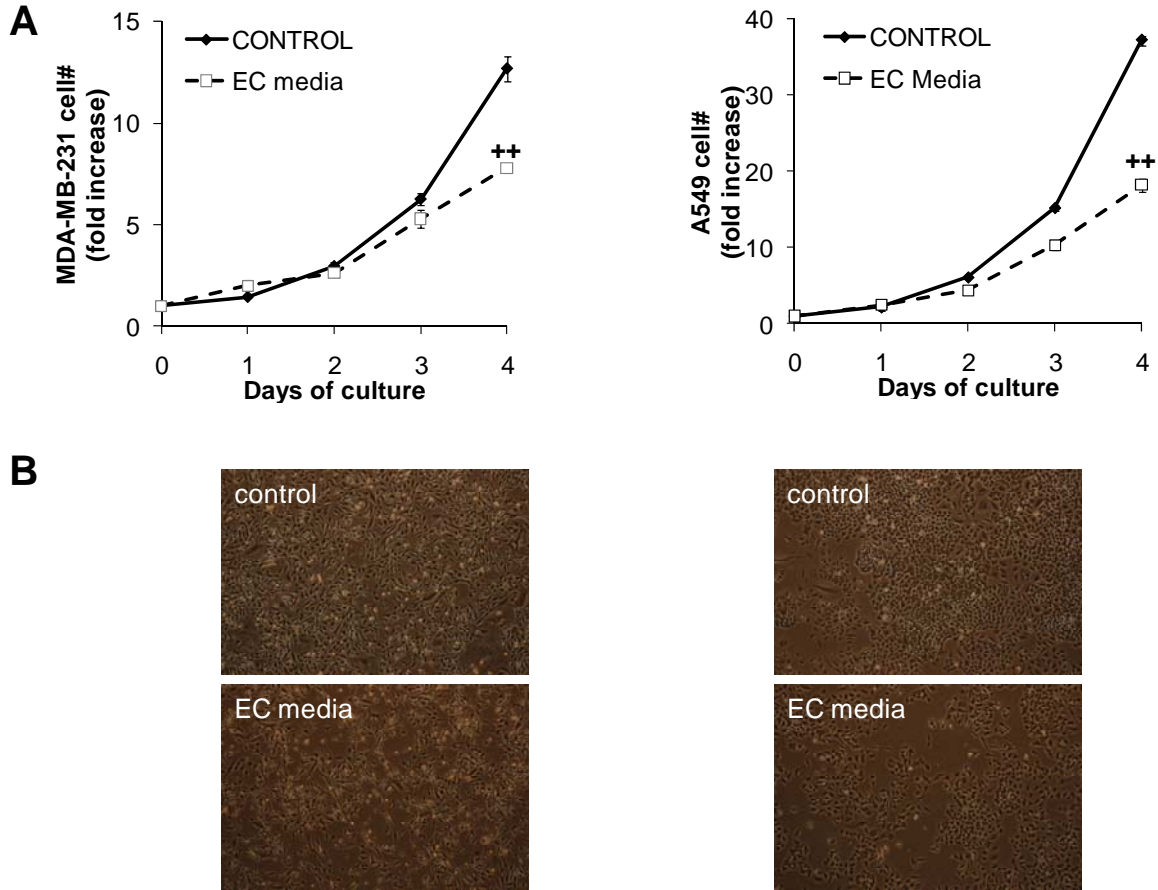
Cells in chamber slides were washed, fixed (10 minutes, 4% paraformaldehyde, room temperature), permeabilized with 0.25% Triton X-100, and incubated with primary antibodies overnight at 4°C. Fluorescently-labeled secondary antibodies were added, along with 1 µg/mL DAPI, for two hours at room temperature in the dark. Cells were then washed, coverslipped (ProLong Gold antifade medium, Invitrogen), and imaged using an epifluorescence microscope (Leica). Images were analyzed using ImageJ. Excised primary tumors and lungs were flash frozen in liquid nitrogen-cooled isopentane. 10-µm frozen sections were cut using a cryotome, fixed for 10 minutes with acetone at -20°C, blocked with serum/BSA/PBS for 45 minutes at room temperature, and stained with appropriate primary and fluorescence-conjugated secondary antibodies as described for cells.

### ***Statistical Analyses***

All experiments were performed at least thrice for validation and each time in triplicate, at minimum; results are expressed as mean±SEM. Comparison of two groups was performed using a student's t-test. Comparison of multiple ( $\geq 2$ ) groups was performed using ANOVA followed by t-tests.  $p < 0.05$  was taken as statistically significant.

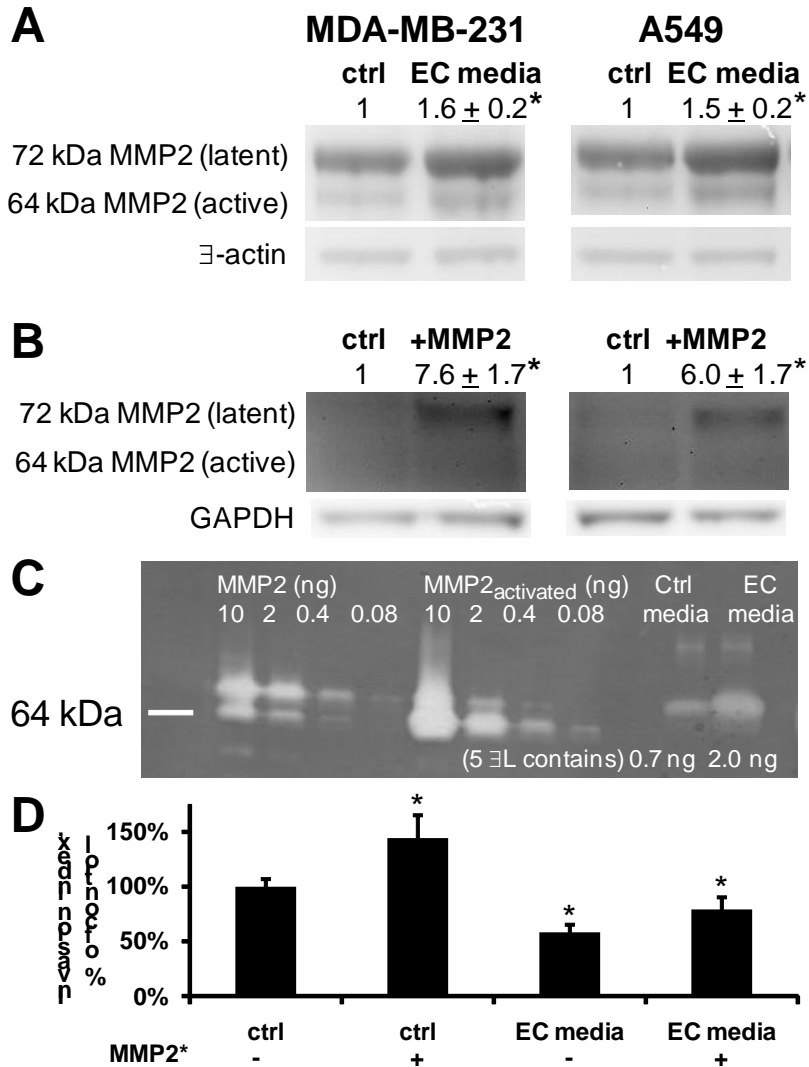
## Supplementary Figures

Figure S1



**Figure S1.** Long-term culture of cancer cells in endothelial cell-conditioned media slows cell growth. (A) Four days after seeding, MDA-MB-231 breast and A549 lung cancer cell number was statistically significantly lower when cultured in media conditioned by quiescent EC compared to cancer cells in control media. Each point represents duplicate measures of at least three different wells. (\*\* =  $p < 0.001$ ) (B) Although cancer cell density and proliferation was affected cell morphology remained unaffected by EC-conditioned media as visualized by phase contrast microscopy.

**Figure S2**



**Figure S2.** Although the secretome of ECs contains a large amount of latent MMP2, it inhibits significantly cancer cell invasiveness. (A) Western blots of whole cell lysates of MDA-MB-231 and A549 cells cultured for 4 days in endothelial cell (EC) conditioned media show an approximately 50% increase in total (latent and active) MMP2 relative to cells cultured in unconditioned media. (B) This effect can be recapitulated by culturing the cells in the presence of recombinant human MMP2. (C) Zymography confirms that EC-conditioned media contains ~ 300 ng/mL more enzymatically-intact MMP2 than unconditioned media. Standard curves of

latent (left) and activated (right) enzyme were used to estimate this value. (D) recombinant MMP2 alone enhances the invasiveness of A549 cells ( $44 \pm 22\%$ ,  $p < 0.05$ ) unless these cells had been cultured previously for 4 days in EC media. EC media inhibits invasiveness ( $41 \pm 16\%$ ,  $p < 0.05$ ) and can even overcome the EC deposition of MMP2 on cancer cells. Invasiveness of cancer cells after exposure to MMP2 and EC conditioned media was suppressed statistically identically to the manner in which media alone acted on cancer cells ( $41 \pm 15\%$  vs.  $22 \pm 13\%$  reduction of invasiveness,  $p = \text{N.S.}$ ).

**Figure S3**

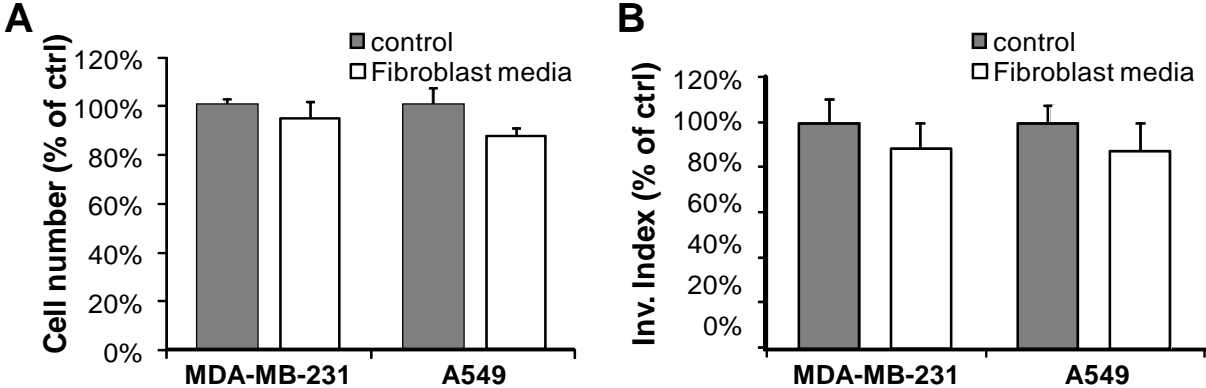


**Figure S3.** Media conditioned by normal fibroblasts have no effect on cancer cell proliferation (A) or invasiveness (B).

**Figure S4**

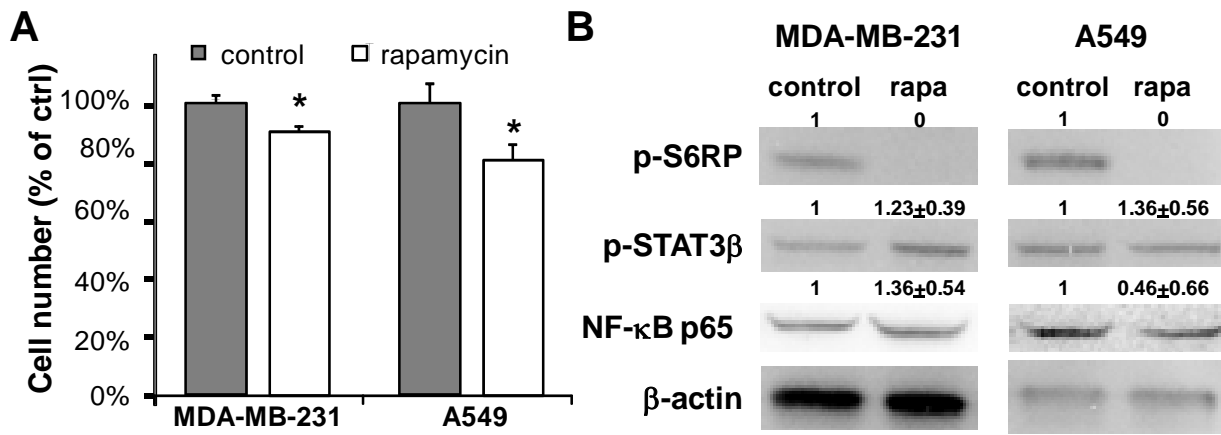


**Figure S4.** Inhibition of one signaling pathway in cancer cells cannot recapitulate EC-mediated regulation of cancer cells. Rapamycin reduced MDA-MD-231 and A549 proliferation 96 hours after exposure by 10% and 17% (A) in concert with almost complete elimination of S6RP phosphorylation but, in contrast to culture in EC-conditioned media, without affecting the phosphorylation of STAT3β or the total levels of NF-κB p65 (B).

**Figure S5**

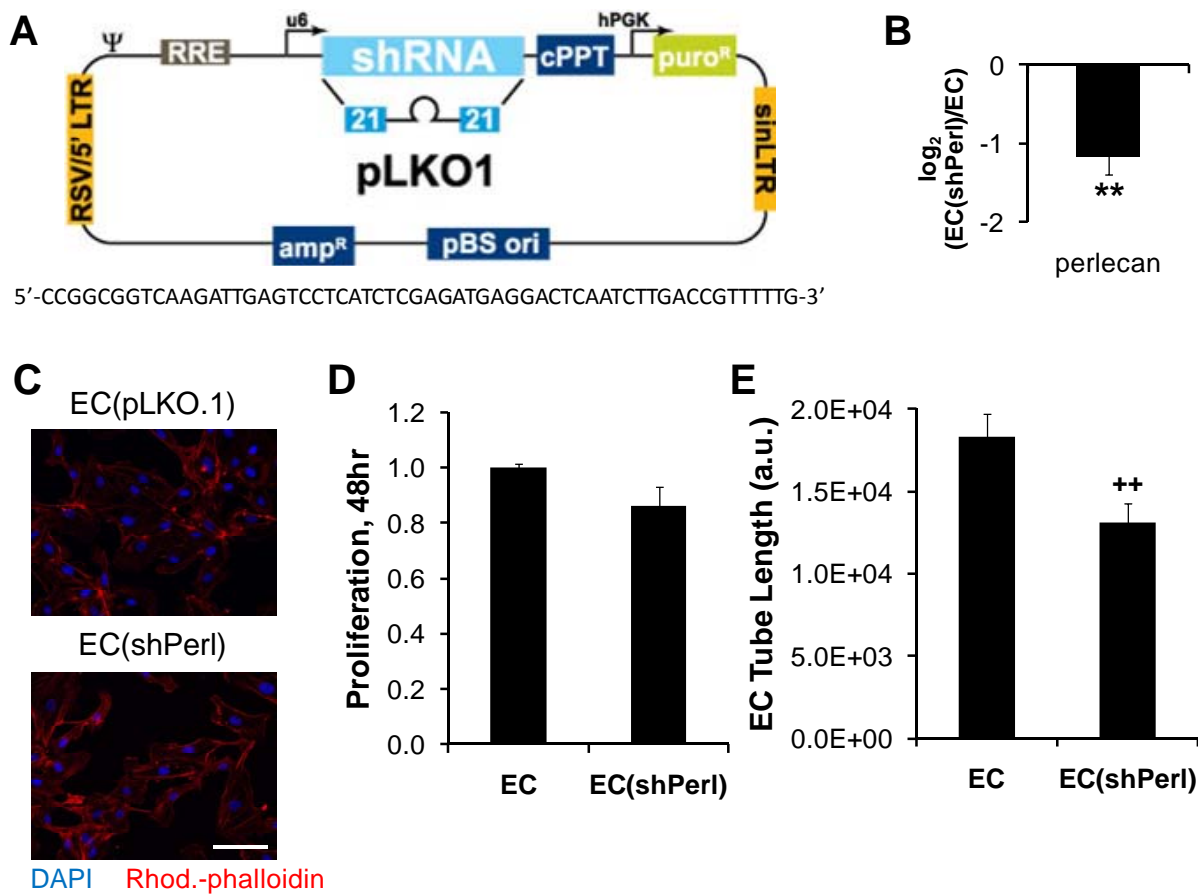


**Figure S5.** Description of perlecan silencing on EC phenotype. (A) Schematic diagram and the shRNA coding sequence of the lentiviral plasmid used for delivery of shRNA targeting perlecan mRNA into ECs. (B) Perlecan mRNA expression in EC is reduced by  $55 \pm 11\%$  ( $p < 0.01$ ) after transduction with a lentiviral plasmid containing shRNA against perlecan, without much affect on EC morphology (C) and without a statistically significant reduction in EC proliferation, (D) and with only modest reduction ( $28 \pm 1\%$ ,  $p < 0.001$ ) of endothelial tube formation (E).

**Figure S6**

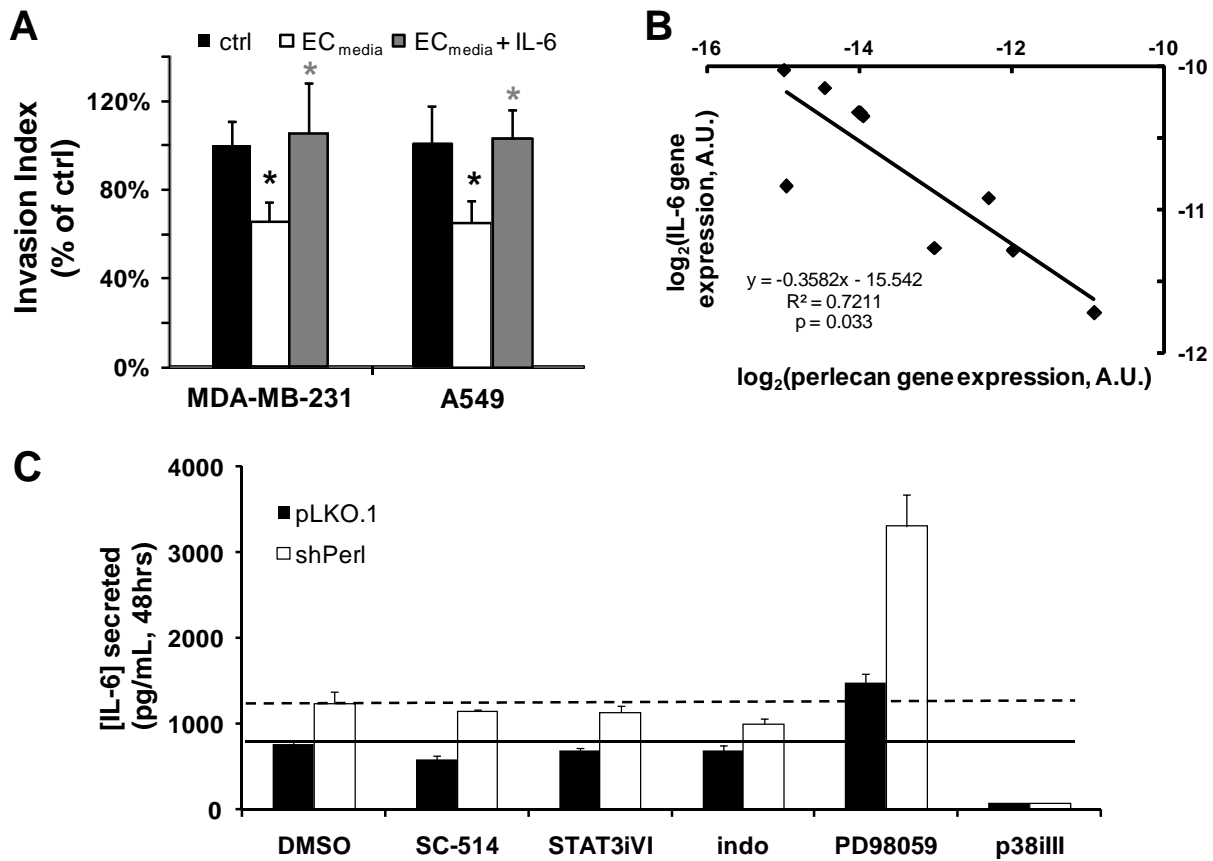


**Figure S6.** Further studies of the perlecan/IL-6 axis in endothelial cells and its role in the regulation of cancer cell invasiveness. (A) The addition of IL-6 (10 ng/mL) to EC media abrogates its ability to suppress cancer cell invasiveness. (B) IL-6 gene expression increases linearly with perlecan silencing. (C) Inhibiting MEK/ERK signaling (PD98059 (Calbiochem) increased IL-6 secretion in both normal and shPerl ECs, whereas inhibiting p38 MAPK signaling (p38iIII, Calbiochem) decreased IL-6 secretion in both EC(pLKO.1) and EC(shPerl). Inhibition of NF- $\kappa$ B signaling (IKK inhibitor SC-514, Calbiochem), STAT3 signaling (STAT3iVI, Calbiochem), cyclooxygenase activity (indomethacin, indo, Sigma) had minimal effect on IL-6 secretion.

Figure S7

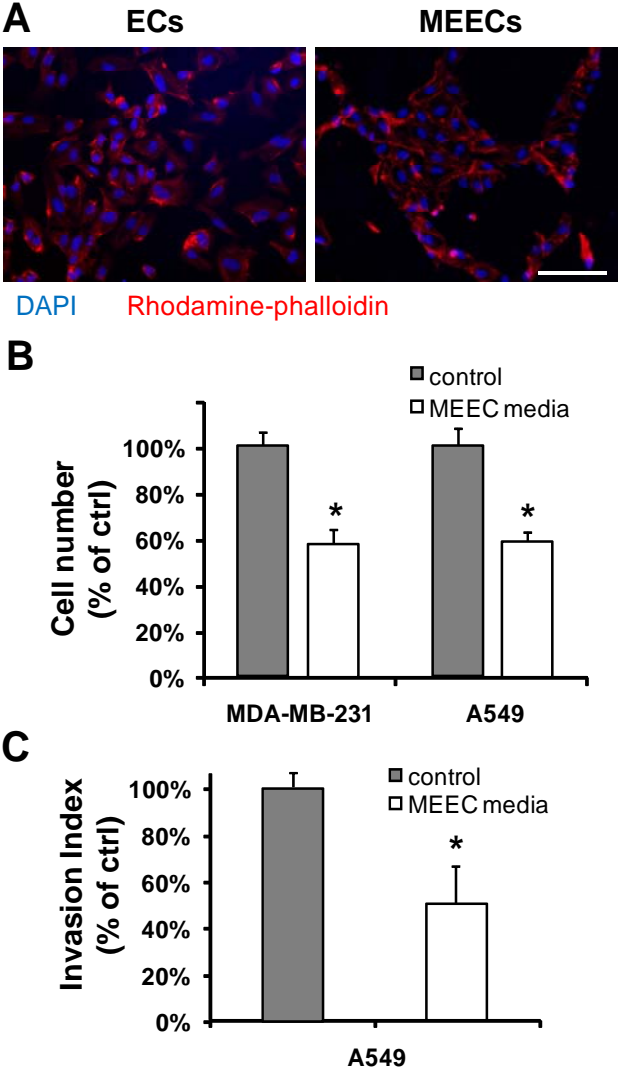


**Figure S7.** MEECs are phenotypically similar to ECs. (A) ECs and MEECs have a similar morphology, as indicated by their actin cytoskeletal structure (scale bar = 50  $\mu$ m). MEECs inhibit cancer cell proliferation (B) and invasiveness (C) to a similar extent as do ECs.

Figure S8

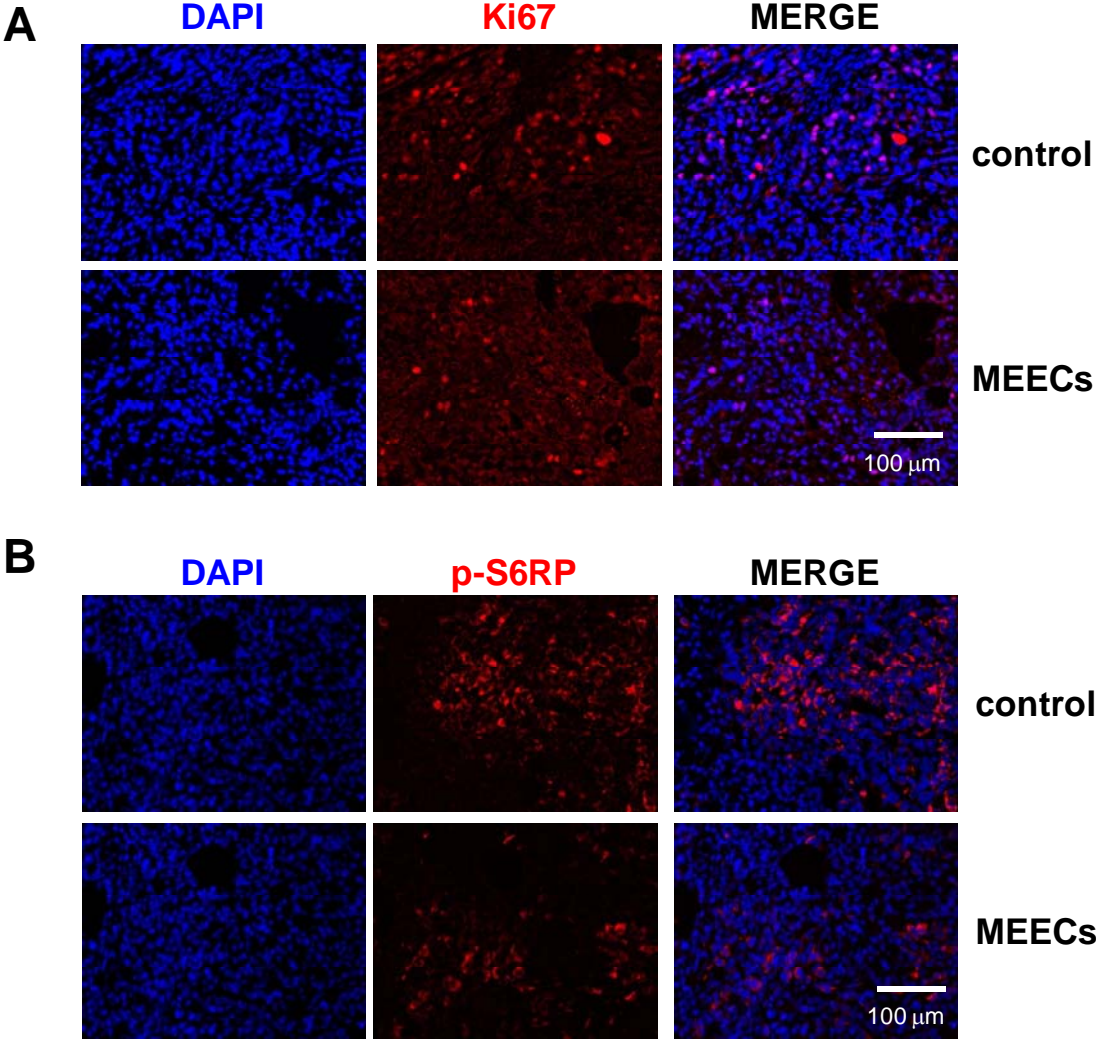
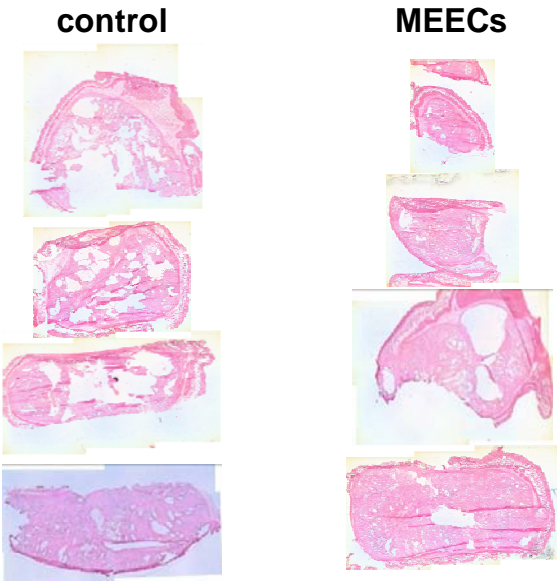


Figure S8. Representative Ki-67 (A) and S6RP (B) staining in control and MEEC-treated A549 xenograft tumors.

**Figure S9**



**Figure S9.** H&E-stained sections from each tumor showing intratumoral cysts.

**Table S1**

	<b>forward 5' - 3'</b>	<b>reverse 5' - 3'</b>
GAPDH	ACAGTCAGCCGCATCTTCTT	TGGAAGATGGTGATGGGATT
MMP2	AACGGACAAAGAGTTGGCAG	GTAGTTGGCCACATCTGGGT
MT1-MMP	TGATAAACCCAAAAACCCCA	CCTTCCTCTCGTAGGCAGTG
TIMP1	GGAATGCACAGTGTTTCCCT	GAAGCCCTTTTCAGAGCCTT
TIMP2	TGATCCACACACGTTGGTCT	TTTGAGTTGCTTGCAGGATG
Perlecan	ATTCAGGGGAGTACGTGTGC	TAAGCTGCCTCCACGCTTAT
IL-6	CACAAGCGCCTTCGGTCCAGTT	TCTGCCAGTGCCTCTTTGCTGC

**Table S1.** List of primers used for qRT-PCR.